Discontinuous Meniscus Location in Tapered Capillaries Driven by Pressure Difference and Dielectrophoretic Forces

Yoav Tsori

Department of Chemical Engineering, Ben-Gurion University of the Negev, P.O. Box 653, 84105 Beer-Sheva, Israel

Received February 4, 2007. In Final Form: March 19, 2007

We calculate the meniscus location in tapered capillaries under the influence of pressure difference and dielectrophoretic forces with and without gravity. We find that the meniscus location can be a discontinuous function of the pressure difference or the applied voltage and that the meniscus can "jump" to one end or another of the capillary. Phase diagrams are given as a function of the pressure and voltage, depending on the geometrical parameters of the system. We further consider a revision of the dielectric rise under dielectrophoretic force in wedge capillaries and in the case of electrowetting, where the dielectrophoretic force is a small perturbation. Finally, we also find discontinuous liquid−gas interface location in the case of liquid penetration into closed volumes.

1. Introduction

The location of the interface between two immiscible liquids or between a liquid and a gas is essential in microfluidic applications, since the meniscus determines the way light is scattered,[1−3] how chemical species interact,[4,5] the way drops are transported in small channels,[6,7] and so forth. Attention must be given to liquid channels or capillaries where the cross section is nonuniform, since liquid channels are never perfectly uniform and, as we show below, this nonuniformity has a strong effect on the meniscus location.[8−10]

Consider a liquid contained in a channel with hard walls and a varying cross section, and suppose that there is a pressure difference ΔP between the two sides of the meniscus. At first glance, it seems that an increase in ΔP will cause the meniscus to move to the point where the Laplace pressure, as determined from the local geometry, equals ΔP, so the meniscus location as a function of ΔP is continuous if the channel is smooth. When a dielectrophoretic force or, indeed, a gravitational force is acting on the liquid at the same time, we find that this naive picture is changed and that the meniscus location becomes a discontinuous function of ΔP. The current case is different from those of refs 9 and 11 in that (i) it takes into account gravity and electrostatic forces, (ii) pressure differences exist even for a flat interface due to an external "pumping", and (iii) the liquid layer is found underneath the solid surface and acts as a big reservoir.

To be concrete, we consider the illustration in Figure 1. A similar wedge-shaped geometry has recently been investigated on homogeneous (miscible) liquid mixtures.[12,13] Here, the meniscus can be a liquid−gas or liquid−liquid interface, and its location is given by h (being negative in part a and positive in part b). The distance between the tilted planes at $h = 0$ is $2R_0$, and α is the tilt angle. In regular capillary rise, h is positive if the wetting angle θ is smaller than $(1/2)\pi$ and is negative if $\theta > (1/2)\pi$. In addition to the gravitational forces and the pressure difference, a dielectrophoretic force is acting: a high-frequency

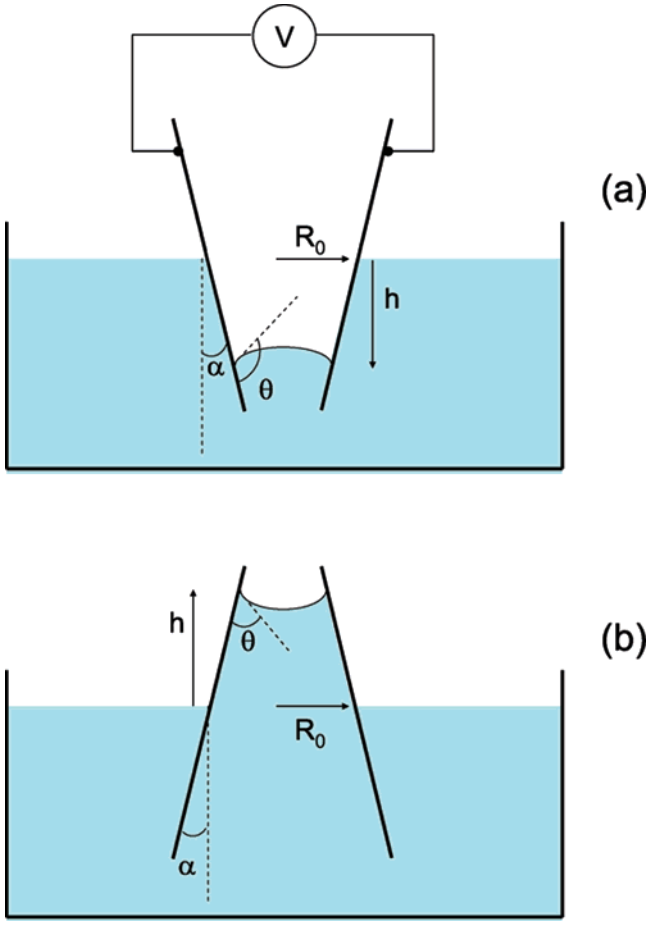

Figure 1. Schematic illustration of a tapered liquid channel made up of two tilted planes, and definitions of parameters. Two of the possible cases are shown: (a) Hydrophobic surface, $\cos\theta < 0$, connected to a voltage supply. The opening angle α is positive, and h is negative. (b) Hydrophilic surface, $\cos\theta > 0$, negative α and positive h.

(1) Beebe, D. J.; Atencia, J. *Nature* **2005**, *437*, 648.
(2) Whitesides, G. M. *Nature* **2006**, *442*, 368.
(3) Psaltis, D.; Quake, S. R.; Yang, C. *Nature* **2006**, *442*, 381.
(4) Janasek, D.; Franzke, J.; Manz, A. *Nature* **2006**, *442*, 374.
(5) deMello, A. J. *Nature* **2006**, *442*, 394.
(6) de Gennes, P. G.; Brochard-Wyart, F.; Quéré, D. *Gouttes, bulles, perles et ondes*; Belin: Paris, 2002.
(7) de Gennes, P. G. *Rev. Mod. Phys.* **1985**, *57*, 827.
(8) Jones, T. B. *J. Appl. Phys.* **1974**, *45*, 1487.
(9) Shuttleworth, R.; Bailey, G. L. J. *Discuss. Faraday Soc.* **1948**, *3*, 16.
(10) Tsori, Y. *Langmuir* **2006**, *22*, 8860.
(11) Parry, A. O.; Wood, A. J.; Rascon, C. *J. Phys.: Condens. Matter* **2001**, *13*, 4591.
(12) Tsori, Y.; Tournilhac, F.; Leibler, L. *Nature* **2004**, *430*, 544. Tsori, Y.; Leibler, L. *Proc. Natl. Acad. Sci. U.S.A.* **2007**, *104*, 7348.
(13) Tsori, Y.; Leibler, L. *Phys. Rev. E* **2005**, *71*, 032101.

10.1021/la7003062 CCC: $37.00
Published on Web 06/21/2007

voltage difference V is imposed across the two tilted planes. The frequency is assumed to be high enough so ionic screening does not occur, and the force exerted on the liquid is dielectrophoretic in nature.

We restrict ourselves to narrow capillaries, where $\kappa R \ll 1$ is satisfied, where $\kappa^{-1} = (\sigma/g\Delta\rho)^{1/2}$ is the capillary length (σ is the interfacial tension, and $\Delta\rho$ is the density difference between the two liquids). In this case, as will be verified below, the height is larger than the radius, $h \gg R$, and the height variations of the meniscus surface are negligible compared to the total height. In mechanical equilibrium, at the contact line, the Laplace pressure is balanced by the hydrostatic pressure

$$P + \frac{\sigma}{r} = P_0 - \Delta\rho g h + \frac{1}{2}\Delta\epsilon E^2(h) \tag{1}$$

where $P_0 - P = \Delta P$ is the pressure difference and r is the inverse curvature given by $r(h) = -R(h)/\cos(\theta + \alpha)$. Here, $2R(h)$ is the surface separation at the meniscus' location and is given by $R(h) = R_0 + h \tan \alpha$. The height-dependent electric field is[13]

$$E(h) = \frac{V}{2\alpha}\frac{\sin \alpha}{R_0 + h \tan \alpha} \tag{2}$$

Finally, $\Delta\epsilon$ is the permittivity difference between the liquid and the gas or between the two liquids.

The electric field has two general effects: (i) it exerts a net dielectrophoretic body force on the liquid and (ii) it changes the contact angle. The exact influence of the electric field thus depends on the applied frequency.[14,15] Unless otherwise stated, we will deal with the high-frequency regime, where the electric field is dielectrophoretic in nature and the contact angle is unaffected by the field. Equation 1 is the basic relation for the meniscus location, and it will be studied in detail for several cases below.

2. No Gravitational Force

The gravitational force is zero if the channel is horizontal, as occurs in many cases, or if $\Delta\rho$ is sufficiently small. In this case, we are faced with the following equation:

$$P + \frac{\sigma}{r} = P_0 + \frac{1}{2}\Delta\epsilon E^2(h) \tag{3}$$

Note that if $\Delta P = 0$ is zero, there is a balance of the dielectrophoretic force against the surface tension, and this leads to some liquid height h where the forces balance. h in this case is a continuous function of the system parameters (e.g., V). Since this is the less interesting scenario, we now assume, without loss of generality, that $\Delta P = P_0 - P > 0$. We obtain the following for the mechanical balance:

$$\frac{1}{8}\Delta\epsilon V^2\left(\frac{\sin \alpha}{\alpha}\right)^2 + \sigma \cos(\theta + \alpha)(R_0 + h \tan \alpha) + \Delta P(R_0 + h \tan \alpha)^2 = 0 \tag{4}$$

This relation can be further cast in the dimensionless form:

$$\frac{1}{8}B\left(\frac{\sin \alpha}{\alpha}\right)^2 + \cos(\theta + \alpha)x + Ax^2 = 0 \tag{5}$$

where

$$x \equiv 1 + \frac{h}{R_0}\tan \alpha \tag{6}$$

and the dimensionless numbers are

$$A = \frac{\Delta P R_0}{\sigma}$$

$$B = \frac{\Delta\epsilon V^2}{\sigma R_0} \tag{7}$$

Let us look at the magnitude of A and B. For a pressure difference $\Delta P = 1$ atm, surface tension $\sigma = 0.1$ N/m, and $R_0 = 1$ mm, we find $A = 10^3$. If $\Delta\epsilon = 10\epsilon_0$ (where ϵ_0 is the vacuum permittivity) and $V = 100$ V, we find $B = 10^{-2}$. Thus, A can be very large while B is typically quite small, and the product is $AB \gtrsim 1$.

Equation 5 is a parabola in the variable x, and x is always positive, because $R_0 + h \tan \alpha > 0$. Let us look at the case of positive A and B but negative $\cos(\theta + \alpha)$; this means that the dielectric liquid is pulled toward higher values of h by the electric field and applied pressure. The minimum of the parabola is at $x_0 = -\cos(\theta + \alpha)/2A$. If B or A is sufficiently small, there are two roots to the equation: an unstable root $x_1 > x_0$ and a stable root $x_2 < x_0$ (see Figure 2a). Figure 2b shows h as a function of the product AB at given α and θ values. There is no solution if A or B is too large, and this occurs when $AB > (AB)_c$, where

$$(AB)_c = 2\cos^2(\alpha + \theta)/[(\sin \alpha)/\alpha]^2 \tag{8}$$

is a critical value of AB. Hence, an increase of AB from below to above $(AB)_c$ leads to a jump of the meniscus from h_0 given by

$$h_0 = -\frac{R_0}{\tan \alpha}\left(1 + \frac{1}{2A}\cos(\theta + \alpha)\right) \tag{9}$$

to the top of the capillary. Relation 8 can be inverted to give a condition for a critical angle θ_c:

$$\theta_c = \arccos\left(\sqrt{\frac{1}{2}AB}\frac{\sin \alpha}{\alpha}\right) - \alpha \tag{10}$$

The meniscus location is changing continuously for $\theta > \theta_c$ and is found at the capillary's top when $\theta < \theta_c$.

The phase diagram is presented in Figure 3 as a function of α and θ for different values of AB. As the value of AB increases from zero, the area below the $\theta_c(\alpha)$ lines (solid curves) increases. This area is where the meniscus is found at the top of the liquid channel, while above it the meniscus location is continuous. Lines (a) and (b) are for $AB = 0.1$ and $AB = 1$, respectively. Curve (c) corresponds to $AB = 2$, and it is the first that touches the limiting diagonal line $\alpha + \theta = \pi$. As AB increases above 2, the line $\theta_c(\alpha)$ overlaps with the $\alpha + \theta = \pi$ line for small values of θ but not for large ones (curve (d) for $AB = 3$). The maximum value of $2\cos^2(\alpha + \theta)/(\sin \alpha/\alpha)^2$ occurs at $\alpha = \theta = (1/2)\pi$. Therefore, from eq 8, we see that there is another special value of AB:

$$(AB)^* = \frac{1}{2}\pi^2 \tag{11}$$

Hence, when $AB > (AB)^*$, the meniscus is at the top for all values of α and θ.

In the following section, we investigate the case of a tapered liquid channel under a gravitational force in addition to the dielectrophoretic force but in the absence of pressure difference.

(14) Jones, T. B. *Langmuir* **2002**, *18*, 4437.
(15) Jones, T. B.; Wang, K.-L.; Yao, D.-J. *Langmuir* **2004**, *20*, 2813.

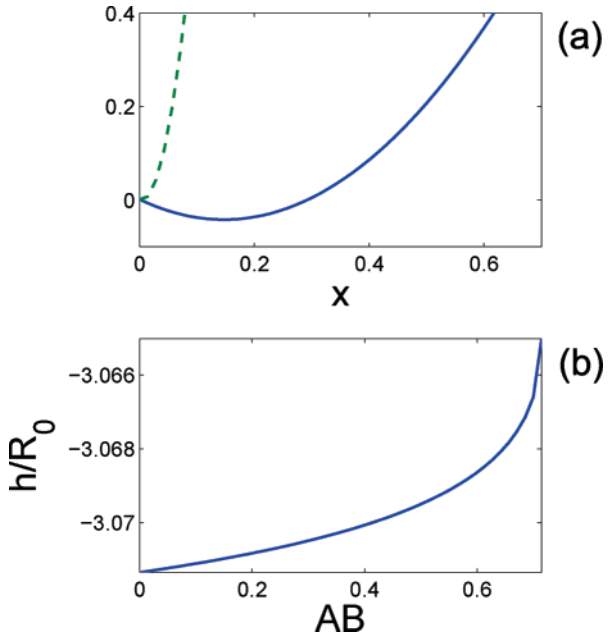

Figure 2. (a) Plot of the left-hand side of eq 5 versus x. If A is large (dashed green curve), there is no real root to the equation. For smaller values of A (solid blue curve), the parabola first descends before it ascends and there are two roots. (b) Plot of the meniscus height h normalized by R_0 as a function of AB. At larger values of AB, $AB > (AB)_c$, the meniscus jumps to the top of the capillary. In both parts, $\alpha = 0.1\pi$, $\theta = 0.6\pi$, $R_0 = 1$ mm, and $(AB)_c = 0.71$.

3. Gravity Effect in the Absence of Pressure Difference

We now turn to the rather complex case where there are dielectrophoretic and interfacial tension forces acting, together with gravity, but no pressure difference. The governing equation reads as follows:

$$\frac{1}{8}\Delta\epsilon V^2\left(\frac{\sin\alpha}{\alpha}\right)^2 + \sigma\cos(\alpha+\theta)(R_0 + h\tan\alpha) = \Delta\rho g h(R_0 + h\tan\alpha)^2 \quad (12)$$

The high-frequency limit of the potential V corresponds to the purely dielectrophoretic case, where θ is simply the zero-field contact angle. In the low-frequency limit, $\omega \to 0$, the dielectrophoretic force vanishes (this is equivalent to setting $V = 0$ above), while $\theta = \theta(V)$ is the voltage-dependent (Lipmann) contact angle.

The gravitational force introduces the capillary length $\kappa^{-1} = (\sigma/g\Delta\rho)^{1/2}$, and this length is used to scale all lengths in the system. The above equation can be expressed using dimensionless lengths as follows:

$$\cos(\alpha+\theta) = f(\bar{h})$$
$$f(\bar{h}) \equiv \bar{R}_0\bar{h} + (\tan\alpha)\bar{h}^2 - \frac{1}{8}\frac{B\left(\frac{\sin\alpha}{\alpha}\right)^2}{1 + \frac{\bar{h}}{\bar{R}_0}\tan\alpha} \quad (13)$$

where

$$\bar{h} = \kappa h, \quad \bar{R}_0 = \kappa R_0 \quad (14)$$

To investigate the field effect, we note that B is usually small and seek solutions with $B \ll 1$. In the absence of an electric field ($B = 0$), eq 13 was recently studied in ref 10, and we give here a brief summary of the main results. We rewrite eq 13 without the B-dependent terms as follows:

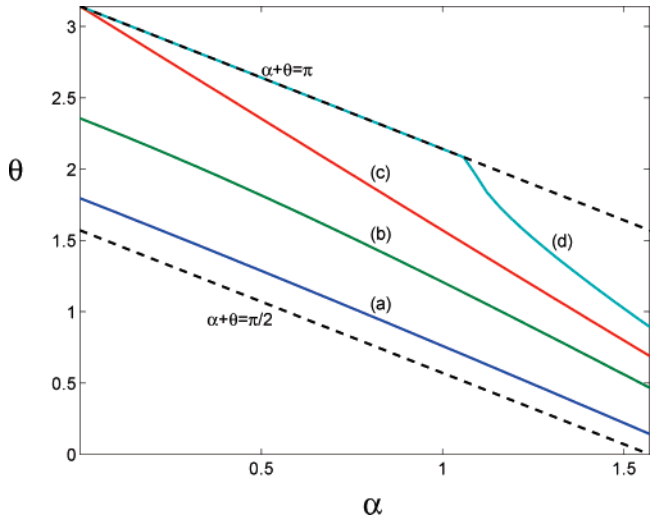

Figure 3. Phase diagram in the $\alpha-\theta$ plane. α and θ are restricted to be between the two diagonal dashed lines $\alpha + \theta = \pi$ and $\alpha + \theta = (1/2)\pi$. The solid line marked as (a), corresponding to $AB = 0.1$, divides the plane into two parts: below it, the meniscus is at the top of the capillary, and above it, h is a continuous function of α and θ. Lines (b), (c), and (d) are the same, but with $AB = 1$, $AB = 2$, and $AB = 3 < (AB)^*$, respectively. At $AB > (AB)^* = (1/2)\pi^2$, the meniscus is at the top, irrespective of α and θ.

$$\cos(\alpha+\theta) = f(\bar{h})$$
$$f(\bar{h}) = \bar{R}_0\bar{h} + (\tan\alpha)\bar{h}^2 \quad (15)$$

$f(\bar{h})$ has a maximum at $\bar{h} = \bar{h}^* = -\bar{R}_0/(2\tan\alpha)$, and its value at the maximum is $f(\bar{h}^*) = -\bar{R}_0^2/(4\tan\alpha)$. Thus, for hydrophilic surfaces ($\cos(\alpha+\theta) > 0$), for small and negative α values, there is a solution to eq 15. If $|\alpha|$ is too large, however, there is no solution: $-\bar{R}_0^2/(4\tan\alpha)$ is smaller than $\cos(\alpha+\theta)$, and the meniscus jumps from

$$\bar{h}^* = -\frac{\bar{R}_0}{2\tan\alpha} \quad (16)$$

to the capillary's end (to the top if $\alpha < 0$ and to the bottom if $\alpha > 0$). The condition for the meniscus' jump is as follows:

$$\cos(\alpha+\theta) = f(\bar{h}^*) = -\frac{1}{4}\frac{\bar{R}_0^2}{\tan\alpha} \qquad \text{no field} \quad (17)$$

Alternatively, the condition can be expressed as a condition for a critical angle $\theta_c(\alpha)$:

$$\theta_c = \arccos(-\bar{R}_0^2/4\tan\alpha) - \alpha \qquad \text{no field} \quad (18)$$

For a negative angle α, the meniscus location is continuous if $\theta > \theta_c$, while the meniscus is at the top for every $\theta < \theta_c$. The system is invariant with respect to the transformation $\alpha \to -\alpha$ and $\theta \to \pi - \theta$. Hence, for a positive value of α, if $\theta > \theta_c$, the meniscus is at the capillary's bottom, and its location is continuously changing for $\theta < \theta_c$. There is a "special" angle α^* given by $\alpha^* = \arcsin(\bar{R}_0^2/4)$. If $-\alpha^* < \alpha < \alpha^*$, the meniscus location as a function of θ is continuous for all θ values.

We now add the field's effect and treat eq 13 perturbatively with small B values. We are looking for the maximum of $f(\bar{h})$

from eq 13. Using $B \ll 1$, we find that

$$\bar{h}^* = -\frac{\bar{R}_0}{2\tan\alpha} - \frac{1}{4}\frac{B[(\sin\alpha)/\alpha]^2/\bar{R}_0}{1 + B[(\sin\alpha)/\alpha]^2\tan\alpha/\bar{R}_0^2} \quad (19)$$

To first order in B, the relation replacing eq 17 is

$$\cos(\alpha + \theta) = -\frac{1}{4}\frac{\bar{R}_0^2}{\tan\alpha} - \frac{1}{4}B\left(\frac{\sin\alpha}{\alpha}\right)^2 \quad (20)$$

Note that, in the preceding derivation, the second term on the right-hand side was assumed to be small compared with the first term. However, as α approaches $(1/2)\pi$, the first term goes to zero, while $\sin\alpha/\alpha$ is finite; in this limit, the dielectrophoretic term dominates and does not represent a small correction anymore, and our derivation fails.

The condition for the critical angle becomes

$$\theta_c = \arccos\left(-\frac{1}{4}\frac{\bar{R}_0^2}{\tan\alpha} - \frac{1}{4}B\left(\frac{\sin\alpha}{\alpha}\right)^2\right) - \alpha \quad (21)$$

Figure 4 summarizes these findings. The zero-field critical value of $\theta(\alpha)$ is shown as dashed lines in Figure 4a, while the solid lines represent the critical angle for the case where $B = 0.3$. At a positive α value, if $\theta < \theta_c$, the meniscus location is continuously changing with θ. Below the diagonal dashed line, h is positive, while $h < 0$ above the dashed line. Above the θ_c line, the meniscus is at the capillary's bottom. Note that the electric field breaks the symmetry of the system: while basically similar behavior appears at negative values of α, the operation $\alpha \rightarrow -\alpha$ and $\theta \rightarrow \pi - \theta$ does not leave the system invariant as it does for the $B = 0$ case.

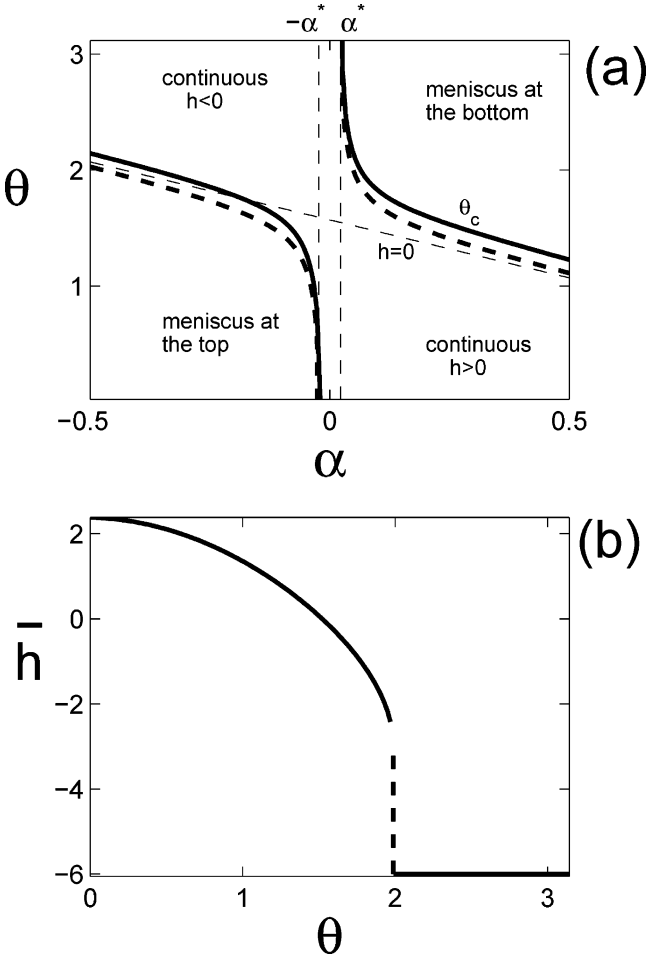

Figure 4. (a) Phase diagram in the $\alpha-\theta$ plane of a liquid in a tapered channel with dielectrophoretic and gravitational forces. The thick dashed lines are θ_c from eq 21 with $B = 0$, and the thick solid lines are for the case where $B = 0.5$. Above θ_c and for positive α, the meniscus is at the capillary's bottom, whereas it is continuously varying below θ_c. For negative α, the meniscus is at the top provided that $\theta < \theta_c$. The thin diagonal dashed line represents the meniscus height $h = 0$; above it, the meniscus is at a negative location, and below it, the meniscus is at a positive location. (b) Normalized meniscus height $\bar{h}$ as a function of θ for a fixed value $\alpha = 0.05$. When θ becomes larger than θ_c (in this case, $\theta_c \simeq 2$), the meniscus jumps to the capillary's bottom. In (a) and (b), we took $\bar{R}_0 = 0.3$.

4. Revision of the Problem of Dielectric Rise

We now consider the case of a liquid dielectric rise in tapered capacitors. We assume that the interfacial tension σ is negligibly small and that there are no imposed pressure differences: $\Delta P = P_0 - P = 0$. The first treatment to this problem was given by T. B. Jones in a classical paper from 1974.[8] The hydrostatic pressure is balanced by the dielectrophoretic force, yielding

$$\frac{1}{8}\Delta\epsilon V^2\left(\frac{\sin\alpha}{\alpha}\right)^2 = \Delta\rho g h(R_0 + h\tan\alpha)^2 \quad (22)$$

Or, expressed differently,

$$\frac{1}{8}\left(\frac{\sin\alpha}{\alpha}\right)^2 = f(\tilde{h})$$

$$f(\tilde{h}) = \tilde{h}(\tilde{R}_0 + \tilde{h}\tan\alpha)^2 \quad (23)$$

where the dimensionless quantities are

$$\tilde{h} = h/L, \quad \tilde{R}_0 = R_0/L \quad (24)$$

and L is given by

$$L = \left(\frac{\Delta\epsilon V^2}{\Delta\rho g}\right)^{1/3} \quad (25)$$

The difference between our derivation and the one by Jones is the expression for the electric field (eq 2), which is more accurate for large angles (α); however, in the limit $\alpha \rightarrow 0$, we expect to recover Jones' results. In the more usual case of a nontapered capillary ($\alpha = 0$), we recover the familiar expression

$$\tilde{h} = \frac{1}{8\tilde{R}_0^2} \quad (26)$$

which is equivalent to

$$h = \frac{\Delta\epsilon V^2}{8\Delta\rho g}\frac{1}{R_0^2} \quad (27)$$

in physical quantities.

Let us concentrate on the case where $\alpha < 0$. As is seen in Figure 5, $f(\tilde{h})$ has an inflection point. There are two extrema located at

$$\tilde{h}_2 = -\frac{1}{3}\frac{\tilde{R}_0}{\tan\alpha}$$

$$\tilde{h}_1 = -\frac{\tilde{R}_0}{\tan\alpha} \quad (28)$$

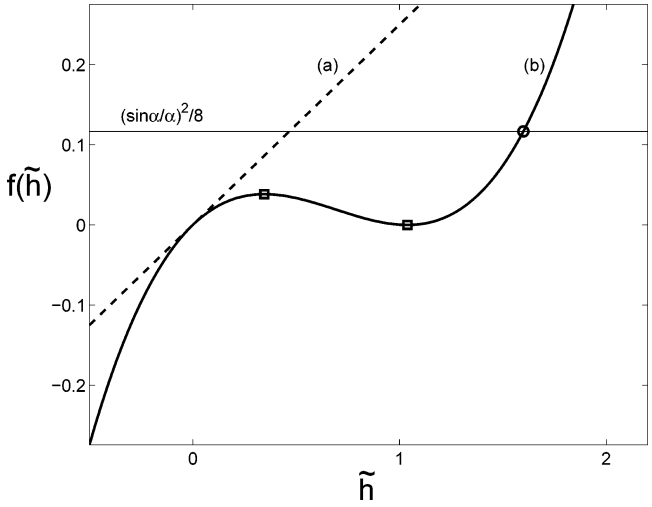

Figure 5. Graphical solution of eq 23. The diagonal dashed line (a) represents $f(\tilde{h})$ for the case where the opening angle is $\alpha = 0$ (regular capillary rise). The curve (b) is $f(\tilde{h})$ for the case where $\alpha = -\pi/7$. The horizontal line is $(1/8)[(\sin\alpha)/\alpha]^2$. Their intersection occurs at the marked circle. As a function of α, the solution may jump from the right branch of $f(\tilde{h})$ to the left one. The two squares mark the extrema $\tilde{h}_1$ and $\tilde{h}_2$ from eq 28 (see text).

Both extrema are positive and are smaller than the maximum height in the capillary, $\tilde{h}_{max} = -\tilde{R}_0/\tan\alpha$. The value of $f(\tilde{h})$ at these extrema is

$$f(\tilde{h}_1) = 0$$

$$f(\tilde{h}_2) = -\frac{4}{27}\frac{\tilde{R}_0^3}{\tan\alpha} \tag{29}$$

The left-hand side of eq 23 represents a horizontal line, and it can cross $f(\tilde{h})$ at the right or left branch. On increasing α from zero, the solution jumps from the right branch to the left one when $(1/8)[(\sin\alpha)/\alpha]^2 = f(\tilde{h}_2)$, that is, when

$$\left(\frac{\sin\alpha}{\alpha}\right)^2 = -\frac{32}{27}\frac{\tilde{R}_0^3}{\tan\alpha} \tag{30}$$

Alternatively, for the critical voltage V_c, we find the following expression:

$$V_c = -\frac{32}{27}\frac{\Delta\rho g}{\Delta\epsilon}\frac{R_0^3}{\tan\alpha\left(\frac{\sin\alpha}{\alpha}\right)^2} \tag{31}$$

Figure 6a shows the phase diagram for the meniscus location. The solid line is $\tilde{R}_0$ from eq 30. At a given negative value of α, if $\tilde{R}_0$ is below the critical line, the meniscus is at the top of the capillary, while above this line the meniscus location is continuous. Figure 6b expresses this behavior in the $\alpha - V$ plane. As V is increased above V_c given by eq 31, the meniscus jumps to the capillary's top. The meniscus location is continuous below it.

In the following section, we find that similarities appear for a liquid channel blocked at one end, because in this case the pressure difference ΔP depends on the meniscus location.

5. Liquid Penetration into Closed Volumes

In this section, we turn to describing the meniscus location in tapered channels where one of the ends is blocked. The interface

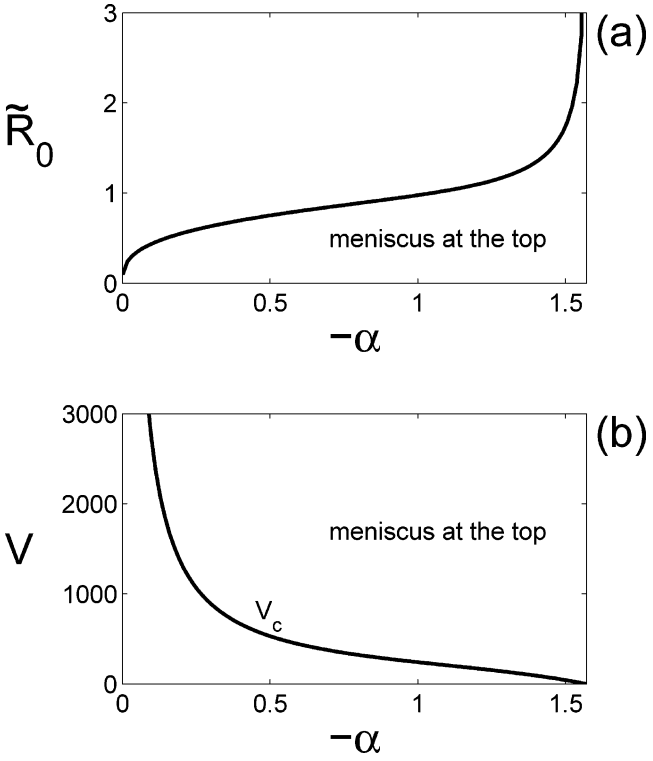

Figure 6. (a) Phase diagram for the liquid rise in tapered capillaries with zero pressure difference ($\Delta P = 0$) and negligible interfacial tension. The opening angle α is assumed to be negative here. At a given value of α, if R_0 is smaller than its value given by eq 30 (solid curve), the meniscus is found at the top of the capillary. (b) Phase diagram in the $\alpha - V$ plane. As V (in volts) is increased above the V_c value given by eq 31 (solid curve), the meniscus jumps to the capillary's top. We took Earth's gravity, the density of water, $R_0 =$ 0.1 mm, and $\Delta\epsilon$ equals five times the vacuum permittivity.

is a gas−liquid interface, as depicted in Figure 7. In the following, we assume that gravity and electric fields are absent, but nonetheless we find that the meniscus location can be discontinuous. The reason for this is the nonlinear dependence of the gas pressure in the area enclosed by the liquid and the walls on the gas volume, and the gas pressure must be balanced by the Laplace pressure.

The liquid channel is wedge-shaped, with large and small opening radii R_2 and R_1, as measured from the imaginary meeting point of the channel walls, and the opening angle is 2α, as defined in Figure 7. Let us call V_0 and P_0 the gas volume and pressure, respectively, just before contact of the liquid channel with the liquid reservoir; P_0 is also the ambient pressure in the liquid. The channel is then brought in contact with the liquid, the liquid pressure is increased by an amount ΔP, and the liquid may penetrate to a distance R inside the capillary. It follows from simple geometry that the maximum gas volume V_0 (i.e., when $R = R_1$) is

$$V_0 = L_z\alpha(R_2^2 - R_1^2) \tag{32}$$

where L_z is its depth in the third dimension (in the page). The total gas volume for $R > R_1$ is

$$V = L_z\alpha(R_2^2 - R^2) \tag{33}$$

Assuming the ideal gas law $P_0V_0 = PV$, we find that the

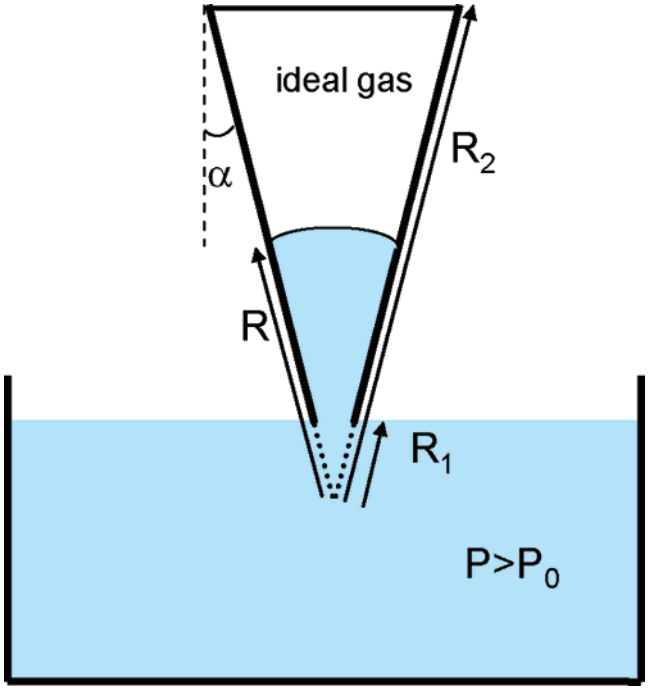

Figure 7. Schematic illustration of liquid penetration into closed volumes. The wedge-shaped channel is closed at one end and is brought into contact with the liquid reservoir. Before contact, the pressure is equal to P_0 everywhere. After contact, the liquid may penetrate into the channel if the outside pressure is increased to $P = P_0 + \Delta P$. The larger and smaller channel radii are R_2 and R_1, respectively, measured from the imaginary meeting point of the walls, and the penetration depth is R.

gas pressure is

$$P = P_0 \frac{R_2^2 - R_1^2}{R_2^2 - R^2} \tag{34}$$

The outside pressure is increased to $P_0 + \Delta P$. We continue in the limit of the very small channel opening, that is, $R_1 \ll R_2(\Delta P/P_0)^{1/2}$ and $R_1 \ll R$, and therefore, eq 3 with $E = 0$ leads to

$$P_0 \frac{R^2}{R_2^2 - R^2} = \frac{\sigma \cos(\alpha + \theta)}{R \sin \alpha} + \Delta P \tag{35}$$

This governing equation can be written using the dimensionless variables

$$x = \frac{R}{R_2}$$

$$A = \frac{R_2 P_0}{\sigma}$$

$$\bar{p} = \frac{\Delta P}{P_0} \tag{36}$$

in the following form:

$$\frac{1}{A}\frac{\cos(\alpha + \theta)}{\sin \alpha} = f(x)$$

$$f(x) = -\bar{p}x + \frac{1}{A}\frac{\cos(\alpha + \theta)}{\sin \alpha}x^2 + (1 + \bar{p})x^3 \tag{37}$$

At this point, we would like to remind the reader that if the ambient pressure is atmospheric, $P_0 = 10^5$ Pa, it follows that $A = P_0 R_2/\sigma \approx 10^4 \gg 1$, where we took $\sigma = 0.1$ N/m and $R_2 = 1$ cm. In the following, we will concentrate on $\bar{p} \ll 1$; however, we will assume $A^{-1} \ll \bar{p}$.

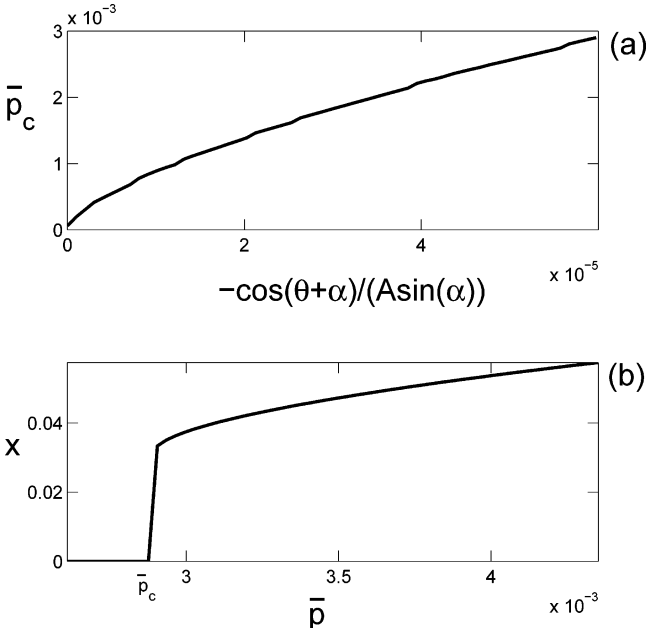

Figure 8. (a) Plot of $\bar{p}_c$, the critical value of the reduced pressure $\bar{p} = \Delta P/P_0$, as a function of $\cos(\alpha + \theta)/(A \sin \alpha)$, where $A = R_2 P_0/\sigma$. $\bar{p}_c$ is computed from eq 40. (b) Scaled meniscus location $x = R/R_2$ as a function of the scaled pressure difference $\bar{p}$. If $\bar{p} < \bar{p}_c$, the meniscus is at $x = 0$; that is, the liquid does not penetrate into the channel. When $\bar{p} = \bar{p}_c$, the meniscus jumps to $x = x_0$ as given by eq 41 with $\cos(\alpha + \theta)/(A \sin \alpha) = -6 \times 10^{-5}$.

We seek the meniscus location $x = R/R_2$ for a given pressure difference ΔP and for hydrophobic channels. This means that we seek the solution of eq 37 for fixed A, negative $\cos(\alpha + \theta)$, and increasing $\bar{p}$. x is nonnegative and is smaller than 1, and the function $f(x)$ descends for small x values and ascends for larger x values. The minimum of $f(x)$ is obtained at x_0 given by

$$x_0 = \left[-\frac{1}{A}\frac{\cos(\alpha + \theta)}{\sin \alpha} + \sqrt{\left(\frac{1}{A}\frac{\cos(\alpha + \theta)}{\sin \alpha}\right)^2 + 3\bar{p}(1 + \bar{p})}\right] \Big/ [3(1 + \bar{p})] \tag{38}$$

and the value at the minimum is $f(x_0)$. When $f(x_0) > \cos(\alpha + \theta)/(A \sin \alpha)$, the meniscus is at $x = 0$; that is, the liquid does not penetrate into the closed volume. If $f(x_0) < \cos(\alpha + \theta)/(A \sin \alpha)$, then the meniscus is at $x > x_0$, as is given by a direct solution of eq 37. The meniscus jumps from $x = 0$ to $x = x_0$ when $f(x_0) = \cos(\alpha + \theta)/(A \sin \alpha)$. This can be expressed by the rather long expression

$$\frac{\cos(\alpha + \theta)}{A \sin \alpha} = \left[2\left(\frac{\cos(\alpha + \theta)}{A \sin \alpha}\right)^3 - 2\left(\frac{\cos(\alpha + \theta)}{A \sin \alpha}\right)^2 \sqrt{\left(\frac{\cos(\alpha + \theta)}{A \sin \alpha}\right)^2 + 3\bar{p}(1 + \bar{p})} - 6\bar{p}(1 + \bar{p})\sqrt{\left(\frac{\cos(\alpha + \theta)}{A \sin \alpha}\right)^2 + 3\bar{p}(1 + \bar{p})} + 9\bar{p}(1 + \bar{p})\frac{\cos(\alpha + \theta)}{A \sin \alpha}\right] / (27(1 + \bar{p})^2) \tag{39}$$

As we mentioned above, we are interested in the limit $A^{-1} \ll \bar{p} \ll 1$, and in this case, we can obtain the following approximate

and much simpler expression for the critical value of the dimensionless pressure $\bar{p}_c$:

$$-\frac{2}{\sqrt{3}}\frac{\bar{p}_c\sqrt{\bar{p}_c(1+\bar{p}_c)}}{3+2\bar{p}_c}=\frac{1}{A}\frac{\cos(\alpha+\theta)}{\sin\alpha} \tag{40}$$

As $\bar{p}$ is increased from zero to $\bar{p}=\bar{p}_c$, the meniscus jumps from $x = 0$ to $x = x_0$, where x_0 is given by

$$x_0 \approx \sqrt{\frac{\bar{p}_c}{3(1+\bar{p}_c)}}-\frac{1}{A}\frac{\cos(\alpha+\theta)/\sin\alpha}{3(1+\bar{p}_c)} \tag{41}$$

Figure 8a shows $\bar{p}_c$ as a function of increasing A^{-1} as given by eq 40. $\bar{p}_c \to 0$ if $A^{-1} \to 0$, and $\bar{p}_c$ increases monotonically with A^{-1}. Figure 8b shows the scaled meniscus location x as a function of $\bar{p}$ at a given value of A. As $\bar{p}$ is increased from zero, x jumps from $x = 0$ to $x = x_0$ at $\bar{p}=\bar{p}_c$ and increases monotonically with a further increase in $\bar{p}$.

We would like to stress that one can also ask the following question: at what value of interfacial tension σ does the meniscus jump for a given value of $\bar{p}$? The expression for A_c as a function of $\bar{p}$ is obtained directly from the inversion of eq 40. In addition, we recall that the ideal gas pressure P_0 is given by $P_0 = nk_BT$, where n is the gas density, k_B is the Boltzmann constant, and T is the absolute temperature. We thus point out that one can hold both ΔP and σ constant while changing the temperature. Again, eq 40 can be used to find a critical temperature T_c for the meniscus jump.

6. Conclusions

In this article, we consider in detail the location of a liquid−liquid or liquid−gas interface in tapered capillaries. The driving forces are external pressure difference, interfacial tension, and electrostatic and gravitational forces.

As one would naively expect, a small change in the external forces usually leads to a small change in the equilibrium interface location. However, as is shown above without exception, due to the nonlinearity of the competing forces, there are critical values of the external parameters: pressure, wetting angle, voltage, and so forth. If the external force is close to its critical value, the equilibrium interface location is discontinuous. This is a rather general phenomenon in capillaries with nonuniform cross sections, and occurs even at small "opening angles" α. In section 2, we considered a capillary with a pressure difference and dielectrophoretic forces and obtained the threshold values of applied voltage or pressure difference to drive the meniscus location discontinuity. In section 3, we studied the liquid rise in capillaries under a weak dielectrophoretic force and gravity. The meniscus jump was discussed in terms of the wetting angle θ and wedge opening angle α. We further looked in section 4 at the classical problem of dielectric rise, but this time in a tapered capacitor. Again, we found that the meniscus location exhibits discontinuities as a function of applied voltage or the geometrical parameters. Finally, in section 5, we considered liquid penetration into closed volumes and once more found a similar transition for the meniscus location as a function of the external driving forces.

The rich behavior found above is certainly relevant to several microfluidic systems, where the control of the liquid−gas or liquid−liquid interface at the small scale is important. A generalization which fully takes into account the frequency dependence of electric fields is a natural extension of the current work and should be explored,[14,15] especially in the context of microfluidic systems.

Acknowledgment. I am indebted to F. Brochard-Wyart and P.-G. de Gennes, with whom I had numerous fruitful discussions and correspondences on the subject. For stimulating comments, I would like to thank A. Marmur and T. B. Jones. This research was supported by the Israel Science Foundation (ISF) Grant No. 284/05.

LA7003062